CellPress

Neuron
Perspective

Rhythms for Cognition: Communication through Coherence

Pascal Fries[1,2,*]
[1]Ernst Strüngmann Institute (ESI) for Neuroscience in Cooperation with Max Planck Society, 60528 Frankfurt, Germany
[2]Donders Institute for Brain, Cognition and Behaviour, Radboud University Nijmegen, 6525 EN Nijmegen, Netherlands
*Correspondence: pascal.fries@esi-frankfurt.de
http://dx.doi.org/10.1016/j.neuron.2015.09.034

I propose that synchronization affects communication between neuronal groups. Gamma-band (30–90 Hz) synchronization modulates excitation rapidly enough that it escapes the following inhibition and activates postsynaptic neurons effectively. Synchronization also ensures that a presynaptic activation pattern arrives at postsynaptic neurons in a temporally coordinated manner. At a postsynaptic neuron, multiple presynaptic groups converge, e.g., representing different stimuli. If a stimulus is selected by attention, its neuronal representation shows stronger and higher-frequency gamma-band synchronization. Thereby, the attended stimulus representation selectively entrains postsynaptic neurons. The entrainment creates sequences of short excitation and longer inhibition that are coordinated between pre- and postsynaptic groups to transmit the attended representation and shut out competing inputs. The predominantly bottom-up-directed gamma-band influences are controlled by predominantly top-down-directed alpha-beta-band (8–20 Hz) influences. Attention itself samples stimuli at a 7–8 Hz theta rhythm. Thus, several rhythms and their interplay render neuronal communication effective, precise, and selective.

Imagine a model of the human brain that is both complete to the point of producing behavior that is indistinguishable from human behavior and detailed to the point of atomistic resolution. This hypothetical model would be an invaluable tool in place of imperfect experimental recordings from living subjects by providing complete downloads from the model. However, those downloaded data would require analysis and interpretation, just like experimental data, before any scientific insight were achieved. Scientific insight is human insight, and human insight into the brain proceeds just as human insight into anything else out there in the world. The world provides a wealth of sensory data, in which regularities, relations, and rules need to be found to arrive at an understanding of the perceived processes. Such an understanding may be referred to as a mental model, which restricts itself parsimoniously to the aspects crucial for capturing the essence of the perceived. It might be characterized as abstract and semantic, and it is certainly incomplete in the sense that it discards the rich initial data for an intuitive or conceptual understanding of generative principles behind the data. To present such a concept of neuronal processing, I will define as ''neuronal representation'' the spatial activation pattern in a group of neurons; as ''neuronal communication'' the transfer of one representation in a presynaptic, or sending, group to a new representation in a postsynaptic, or receiving, group; and as ''neuronal computation'' the transformation that happens between the representations. This illustrates the central role of communication as the process that implements computation and thereby creates new representations.

Neuronal communication has classically been conceived of as being determined by structural anatomical connectivity and by activity-dependent changes to the anatomical (ultra)structure of the connection. I propose that even in the absence of changes in (ultra)structural connectivity, neuronal synchronization as an emergent dynamic of active neuronal groups has causal consequences for neuronal communication. If neuronal communication depends on neuronal synchronization, then dynamic changes in synchronization can flexibly alter the pattern of communication. Such flexible changes in the brain's communication structure, on the backbone of the more rigid anatomical structure, are at the heart of cognition.

Communication through Coherence

Because the main thrust of the concept is that neuronal communication is subserved by neuronal synchronization, often quantified by the coherence metric, I have named the concept ''Communication through Coherence,'' or CTC. I formulated the CTC hypothesis 10 years ago (Fries, 2005) and aim here to provide a revised formulation of CTC that takes into account the plethora of CTC-relevant data, which has been generated in the meantime, and that further distils the essence of CTC.

The Essence of CTC

Here are the essential propositions of the CTC hypothesis: An activated neuronal group tends to engage in rhythmic synchronization. Rhythmic synchronization creates sequences of excitation and inhibition that focus both spike output and sensitivity to synaptic input to short temporal windows. The rhythmic modulation of postsynaptic excitability constitutes rhythmic modulations in synaptic input gain. Inputs that consistently arrive at moments of high input gain benefit from enhanced effective connectivity. Thus, strong effective connectivity requires rhythmic synchronization within pre- and postsynaptic groups and coherence between them, or in short—communication requires coherence. In the absence of coherence, inputs arrive at random phases of the excitability cycle and will have

a lower effective connectivity. A postsynaptic neuronal group receiving inputs from several different presynaptic groups responds primarily to the presynaptic group to which it is coherent. Thereby, selective communication is implemented through selective coherence.

The fundamental proposition, that a postsynaptic rhythm modulates input gain, has received direct experimental support. When optogenetic stimulation is used to drive fast-spiking interneurons in somatosensory cortex with a 40 Hz pulse train, the network resonates at gamma frequency, and the precise timing of vibrissa deflections relative to the pulse train affects both neuronal (Cardin et al., 2009) and behavioral (Siegle et al., 2014) responses. Similarly, when a weak sustained muscle contraction induces a corticospinal beta rhythm, transcranial magnetic stimulation pulses applied to motor cortex lead to muscle responses that depend on the phase of stimulation in the beta rhythm (van Elswijk et al., 2010). Note that the transmission of spikes from one area to the next does not only depend on coherence between the areas but also on synchronization within the sending area, as has been demonstrated, e.g., between areas V1 and V2 (Jia et al., 2013a; Zandvakili and Kohn, 2015).

The subsequent proposition, that strong effective connectivity requires coherence between pre- and postsynaptic groups, has also been supported. One study investigated the relation between the effective connectivity and the phase relation for pairs of recording sites in visual cortex of awake cats and monkeys (Womelsdorf et al., 2007). For each trial, the phase relation between gamma rhythms at the two recording sites was determined, and trials were sorted accordingly into phase-relation bins. Across all trials within a phase-relation bin, effective connectivity was then determined. This showed that effective connectivity depends on the phase relation. Effective connectivity is maximal for the phase relation at which the two sites typically synchronize. Phase relations supporting interactions between the groups precede those interactions by a few milliseconds, consistent with a mechanistic role.

The final proposition, that selective communication is implemented through selective coherence, has received experimental support from studies using selective visual attention or selective movement intention. One study tested this prediction in the human motor system, assessing activity from bilateral motor cortices with magnetoencephalography and corresponding spinal activity through electromyography of bilateral hand muscles (Schoffelen et al., 2011). During bimanual wrist extension, each motor cortex showed coherence with its contralateral hand muscle. One of the hands was cued as the response hand to report an unpredictable visual go cue. The corticospinal connection that effectuated the subsequent motor response showed enhanced corticomuscular coherence in the gamma-band (40–47 Hz). This effect was observed in the absence of changes in motor output or changes in local cortical gamma-band synchronization. Thus, selective movement intention is implemented by selective gamma-band coherence. Enhanced corticospinal gamma-band coherence during movement preparation correlates closely with shortened reaction times (Schoffelen et al., 2005). Yet probably the most compelling evidence for selective communication through selective coherence comes from studies of selective visual attention, during which two neuronal groups in a lower visual area compete to communicate with one target group in a higher visual area. These studies will be discussed in detail below.

Challenges for the Original CTC Hypothesis

While there is substantial experimental support, some studies posed challenges to the original CTC formulation that motivated the new CTC formulation. If the two communicating neuronal groups are bidirectionally coupled, I originally proposed zero-phase synchronization (see Figure 3 of Fries, 2005). To cope with increasing delays for increasingly distant groups, I considered lower frequencies. However, recent studies have demonstrated that neuronal groups in widely separated areas can be coherent in the gamma band, i.e., at a relatively high frequency (Bastos et al., 2015a; Bosman et al., 2012; Gregoriou et al., 2009). At the same time, it became clear that even though the areas are bidirectionally coupled, this gamma-band coherence does not occur at zero phase, but with a systematic delay, i.e., with a directedness (Bastos et al., 2015b; Bosman et al., 2012; Gregoriou et al., 2009; Grothe et al., 2012; Jia et al., 2013a; Zandvakili and Kohn, 2015). I had originally suggested such delayed coherence, consistent with a directed entrainment, if the presynaptic group projects unidirectionally to the postsynaptic group. In the new CTC formulation, I suggest that unidirectional entrainment occurs separately in both directions of a bidirectional communication link, as I will explain in more detail below.

A second challenge to the original CTC came from the fact that it had not specified precisely how postsynaptic excitability varies with phase. Mathematical implementations of CTC that assume a sinusoidal oscillation and a linear relation between phase and excitability show that presynaptic groups, which are incoherent to the postsynaptic group, might still have a substantial impact (Akam and Kullmann, 2012). The new CTC proposes that excitability is modulated by rhythmic synchronization in a way that is neither sinusoidal nor linear, in agreement with mathematical models entailing spiking excitatory and inhibitory neurons (Börgers and Kopell, 2008; Cannon et al., 2014; Gielen et al., 2010).

The New CTC

I will illustrate the new CTC, from here on mostly referred to just as CTC, for the case of visual cortical gamma-band synchronization. When visual cortex of an awake and attentive subject is activated by an appropriate stimulus, the activated neurons engage in rhythmic synchronization in the gamma-frequency band (30–90 Hz) (Fries et al., 2001; Gray et al., 1989). This holds during natural viewing (Figure 1; Boxes 1 and 2) (Brunet et al., 2015). During the gamma cycle, excitatory neurons trigger local inhibitory neurons within about 3 ms (Buzsáki and Wang, 2012; Csicsvari et al., 2003; Fries et al., 2007; Hasenstaub et al., 2005; Salkoff et al., 2015; Vinck et al., 2013). When the ensuing inhibition of the local network decays, the gamma cycle starts again with a new round of excitatory neuron spiking. Thus, there is only a 3 ms window for excitation, whereas the longer rest of the gamma cycle is dominated by inhibition (Figure 2A). The spikes travel from the presynaptic neurons, through their anatomical projections, to the postsynaptic neurons, where they trigger excitatory neuron spiking followed by inhibitory neuron spiking. The ensuing inhibition essentially closes the door in front of other inputs, because it strongly reduces their synaptic input gain.

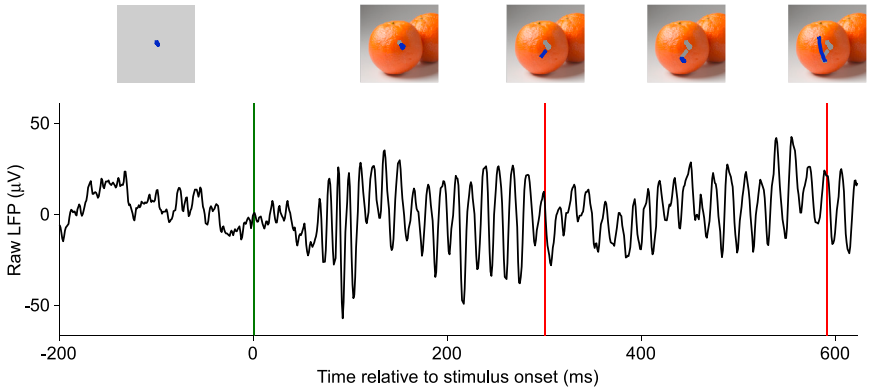

Figure 1. Natural Viewing Induces a Gamma-Band Rhythm in Visual Cortex
Raw LFP trace recorded as the voltage between two neighboring electrocorticographic electrodes on primary visual cortex of an awake macaque monkey during one visual exploration of the photograph of two oranges (adapted and modified from Brunet et al., 2015). Green vertical line indicates stimulus onset, red vertical lines indicate saccades. Insets show the stimulus and superimposed the eye position trace around that time point in blue, and the eye position trace during this exploration so far in gray. Prior to stimulus appearance and free viewing, the monkey fixated on a small central dot.

The unequal duty cycle of short excitation followed by longer inhibition leads to a nonsinusoidal gain modulation (Figure 2B), and the nature of inhibition, involving perisomatic shunting inhibition (Buzsáki and Wang, 2012), leads to a nonlinear gain modulation. If time constants are similar between entrained pre- and postsynaptic networks, the next round of synaptic inputs from the presynaptic network will be timed to the moment when inhibition in the postsynaptic network decays. This is because local excitation triggers local inhibition and thereby starts a few-millisecond timer corresponding to the inhibitory time constant. At the postsynaptic network, excitatory inputs arrive with a delay, which starts the local timer in the postsynaptic network with a corresponding delay. With precisely the same delay, the next round of excitation arrives. This entrainment of the postsynaptic group to the rhythmic input from the presynaptic group automatically sets up a phase relation that is optimal for CTC, as has been highlighted in mathematical models (Börgers and Kopell, 2008; Cannon et al., 2014; Gielen et al., 2010).

In the new CTC formulation, I propose that entrainment with delay is the general mechanism that sets up phase relations subserving CTC, both for unidirectional communication and for bidirectional communication. Bidirectional communication is implemented separately for the two directions, via unidirectional entrainment per direction. Anatomical data actually show that for each direction of communication, the communicating brain areas have specialized neuronal groups, i.e., a given brain area has neurons receiving inputs and different neurons sending outputs (Felleman and Van Essen, 1991; Markov et al., 2014). Thus, the new CTC takes anatomical data on interareal projections more closely into account and resolves the abovementioned challenge arising from observed interareal delays. In addition, systematic investigations of directed interareal influences as a function of frequency revealed that influences in the two directions predominate in distinct frequency bands (Bastos et al., 2015a), as explained in detail below.

The new CTC addresses challenges to the original CTC, but one of the appealing predictions of the original CTC appears at first to be lost with this revision. If, as originally assumed, delays between sending and receiving groups are negligible, coherence increases effective connectivity between the coherent groups in both directions. That is, feedback from the receiving group is likely to be more effective at the coherent sending group than at the noncoherent sending group, even if it is anatomically directed to both (Fries, 2005). Thus, CTC might render anatomically nonselective feedback functionally selective to the appropriate sending group. If, as we now point out, delays are not negligible, both feedforward and feedback signaling will incur some delay. In the sending cortical column, re-entrant feedback inputs will arrive several milliseconds after feedforward outputs have been sent. Those re-entrant feedback inputs can only be coherent with a delayed version of the original output. Intriguingly, such delayed versions have been described. Single neurons in supragranular layers of macaque area V1 show visually induced gamma-band synchronization with a systematic delay of approximately 1 ms per 100 micron shift toward the cortical surface (Livingstone, 1996). Recently, laminar current-source-density analysis revealed that this gamma delay extends from layer 4 toward both supra- and infragranular layers (Figure 3A) (van Kerkoerle et al., 2014). Thus, interlaminar delays might delay the supra- and infragranular gamma phase such that reentrant feedback arrives at the excitable phase of the same, delayed,

Box 1. Current Status of the Field

- Rhythmic synchronization, including gamma-band synchronization, is widespread across the nervous system and across species.
- Different rhythms coexist and are often synchronized to each other or nested into each other.
- Gamma and beta rhythms modulate input gain, and their coherence subserves effective connectivity.
- Rhythmic synchronization in different frequency bands is highly structured across areas, layers, and the corresponding projections.
- Patterns of synchronization change dynamically with stimulation and behavioral context in a way that strongly suggests that selective coherence implements selective communication.

Box 2. Future Directions

- Does rhythmic synchronization, in particular gamma-band synchronization, occur generally in active neuronal groups, also under fully natural conditions?
- Can we experimentally manipulate neuronal synchronization, while leaving other aspects of neuronal activity unchanged, and show effects on neuronal communication?
- Through which cell types and mechanisms do top-down influences affect the strength and frequency of gamma-band synchronization?
- Cortical inhibition is very local, leading to local gamma rhythms; thalamic inhibitory neurons are collected and linked in the thalamic reticular nucleus. Does this allow only one gamma across the thalamus, which needs to be entrained for cortical signal propagation?

gamma cycle (Figure 3B) (Bastos et al., 2015b). Note that interareal anatomical projections have laminar origins and targets that are consistent with the pattern of gamma flow suggested in Figure 3 (Felleman and Van Essen, 1991; Markov et al., 2014). For pairs of areas that are hierarchically very distant, reentrant feedback would arrive too late to hit a matching phase. Intriguingly, we found that for those area pairs, gamma-band influences exist essentially only in the feedforward direction, as discussed in more detail below (Bastos et al., 2015a, 2015b).

In the following, I will argue that gamma-band coherence establishes a communication protocol that is effective, precise, and selective, with one section devoted to each of these three aspects. In two further sections, I will discuss the differential roles of gamma and alpha-beta rhythms in feedforward versus feedback signaling and the role of the theta rhythm in attentional sampling.

Gamma-Band Coherence Renders Communication Effective

The gamma rhythm results in a rapid succession of excitation and inhibition, and this is likely necessary to activate postsynaptic neurons. A typical cortical neuron receives inputs from thousands of neighboring neurons. Among those input neurons, network excitation is faithfully tracked by network inhibition (Renart et al., 2010). Therefore, individual neurons typically receive excitation and inhibition in a balanced way (Haider et al., 2006; Shu et al., 2003), including neurons in awake monkey visual cortex during visual stimulation (Tan et al., 2014). Network excitation drives network inhibition with a small delay. During gamma-band synchronization, this delay has been found to be around 3 ms (Atallah and Scanziani, 2009; Csicsvari et al., 2003; Fries et al., 2007; Hasenstaub et al., 2005; Vinck et al., 2013). I suggest that the gamma rhythm generates fluctuations in network excitation and inhibition that are sufficiently rapid, such that excitation can essentially temporally escape its ever chasing inhibition. The gamma rhythm concentrates inhibition to certain parts of the gamma cycle, which appears necessary to provide moments devoid of inhibition that allow postsynaptic neurons to spike at all (Tiesinga et al., 2004). An important type of inhibition is exerted by parvalbumin-positive (PV) interneurons and is targeted to the soma and perisomatic region, where it can powerfully antagonize and shunt dendritic excitation (Buzsáki and Wang, 2012). If this powerful shunting arrived in a temporally unstructured manner, it would prevent postsynaptic spiking at almost all times. Spiking is enabled by temporally focusing shunting to certain time periods, while leaving others devoid of it (Tiesinga et al., 2004). This time-sharing is achieved by the gamma rhythm, which focuses perisomatic inhibition in one part of the gamma cycle, and thereby leaves another part free for neurons to respond to excitatory input. This excitatory phase of the gamma cycle sees decaying inhibition and a temporally focused rise in excitation (Hasenstaub et al., 2005; Salkoff et al., 2015; Vinck et al., 2013). Such synchronized excitation in turn generates rapid postsynaptic depolarization, ideal to trigger spikes (Azouz and Gray, 2003).

I would like to speculate that the rapid balancing of network excitation by inhibition reduces the postsynaptic impact of neurons, whose spike rate is modulated by the alpha rhythm. The alpha rhythm is strong in cortex that is not activated by a stimulus and/or not addressed by top-down influences like attention (Fries et al., 2008; van Ede et al., 2011; Worden et al., 2000). It has therefore been suggested that the alpha rhythm provides inhibition (Jensen and Mazaheri, 2010). Yet inhibition is involved in all classical EEG rhythms, including the gamma rhythm. The crucial characteristic of alpha seems to be that it blocks the communication of local activity to connected neuronal groups (van Dijk et al., 2008; Zumer et al., 2014). I suggest that the rapid balancing, which renders gamma ideal for neuronal communication, likely renders alpha ideal to preclude communication. In the gamma cycle, excitation rises within few milliseconds, fast enough to lead to postsynaptic depolarization before inhibition terminates it. By contrast, in the alpha cycle, excitation rises over the course of about 50 ms, while inhibition likely follows with the same 3 ms delay; in fact, the spiking of putative excitatory and inhibitory V4 neurons does not show a significant phase shift in the alpha cycle (Vinck et al., 2013). Thus, alpha might be slow enough, such that network excitation cannot escape network inhibition, which cancels postsynaptic effects and renders local activity functionally invisible to remote projection targets. This might allow holding local representations "on-stock" for flexible access by top-down selection mechanisms.

Gamma-Band Coherence Renders Communication Precise

Gamma-band coherence renders communication not only effective but also precise. The gamma rhythm times the inhibition in the postsynaptic group to vanish just before another round of synaptic inputs arrives, and it focuses those synaptic inputs to arrive simultaneously. This synchronous arrival of synaptic inputs is an important component of a precise communication protocol.

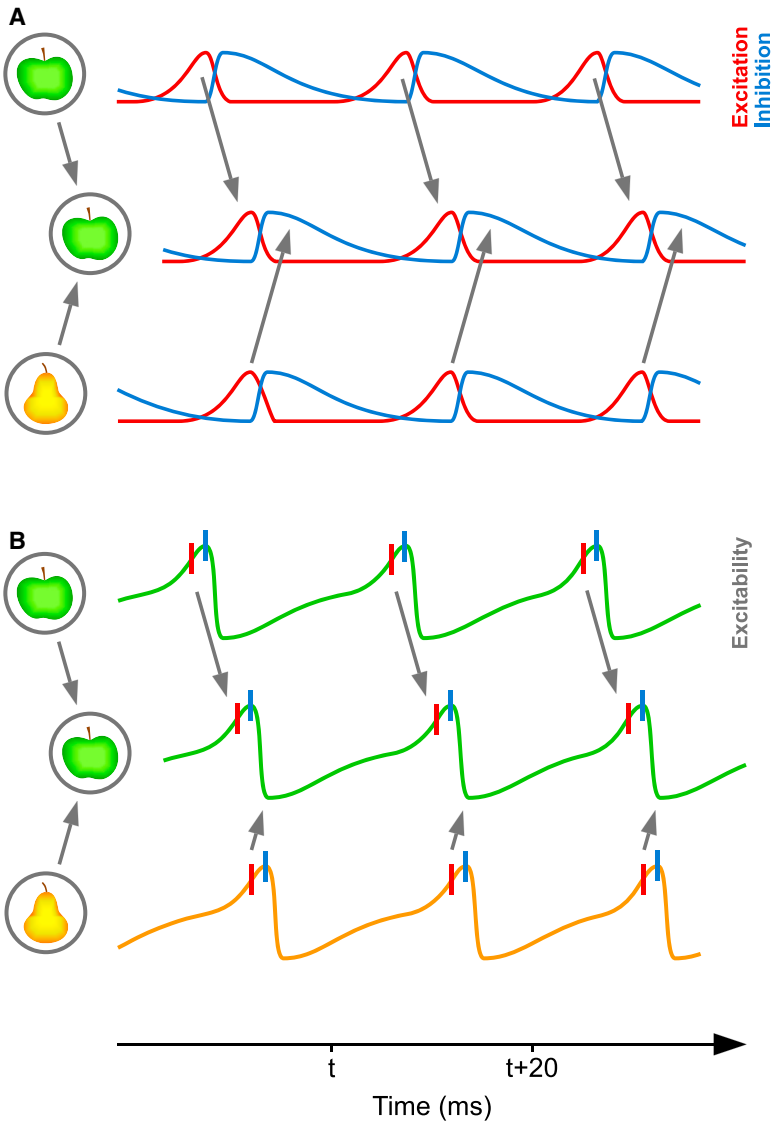

Figure 2. Communication through Coherence

(A) Two presynaptic neuronal groups in a lower visual area provide input to a postsynaptic neuronal group in a higher visual area. The lower groups represent two visual stimuli, an apple and a pear. In each neuronal group, network excitation (red) triggers network inhibition (blue), which inhibits the local network. When inhibition decays, excitation restarts the gamma cycle. The gamma rhythm of the apple-representing presynaptic group has entrained the gamma rhythm in the postsynaptic group. Thereby, the apple-representing presynaptic group can optimally transmit its representation, whereas the pear-representing presynaptic group cannot transmit its representation.

(B) A simplified illustration in which network excitation and inhibition are combined into network excitability. Red vertical lines indicate excitatory neuron spiking and blue vertical lines inhibitory neuron spiking.

The CTC protocol conveys a neuronal representation manifest in the spatial pattern of spike rates in the presynaptic neuronal group. This presynaptic spike rate pattern translates into a spatial activation pattern among the synaptic inputs to the postsynaptic group. The synaptic input pattern, multiplied by the pattern of synaptic strengths, determines the level of postsynaptic depolarization and subsequent spike rate. The spike response should ideally be a precise function of the neuronal representation conveyed by the active set of synaptic inputs. Synaptic currents (at least the dominant AMPA- and $GABA_A$-receptor-mediated currents) decay within a few milliseconds. If synaptic inputs were jittered, even by merely a few milliseconds, this would substantially compromise the precision of the postsynaptic response, i.e., the degree to which it is determined by the presynaptic spatial spike rate pattern. By decreasing such jitter, CTC mechanisms likely increase postsynaptic response precision.

Essentially, CTC renders interneuronal communication pulsatile, because communication happens only during a relatively small fraction of the synchronization cycle. Pulsatile communication results in pulsatile computation and a pulsatile postsynaptic neuronal representation. An ideal test case of a neuronal stimulus representation is the orientation selectivity of primary visual cortex. A recent study investigated single neurons in awake monkey V1 with regard to the orientation selectivity of their firing rate responses. Orientation selectivity was calculated separately for spikes occurring at different times in the gamma cycle (Figure 4) (Womelsdorf et al., 2012). The gamma cycle was subdivided into several phase bins. Spikes occurring close to the gamma phase to which spikes synchronized on average showed stronger orientation selectivity in their spike rates than spikes occurring at other times. These data suggest that the neuronal representation of visual stimulus orientation pulsates with the gamma cycle. Of course, spike rates themselves pulsate with the gamma cycle, and the study controlled that the pulsating neuronal representation was not a trivial consequence of pulsating spike counts. Thus, these results argue against the often-practiced distinction (and rivalry) between a rate code and a synchrony code, but rather for an integration of those schemes (Ainsworth et al., 2012). Specifically, the results suggest a gamma-rhythmic pulsatile rate code, in which the spatial pattern of spike rates holds representations, yet only during short temporal windows in the gamma cycle.

While gamma-band synchronization primarily aligns the spike output of a neuronal group in time, this alignment contains further fine temporal structure (Havenith et al., 2011; Vinck et al., 2010, 2013). In visual cortex, neurons spike earlier in the gamma cycle when they are driven by stimuli closer to their preferred stimulus (Vinck et al., 2010). Thereby, in the cortical stimulus selectivity map, a given stimulus results in a systematic gamma wave of spiking, sweeping from the more to the less strongly activated columns. Postsynaptically, the synaptic inputs from more strongly activated neurons will arrive earlier and will thereby have a larger influence before inhibition curtails further effects (Börgers and Kopell, 2008; Cannon et al., 2014).

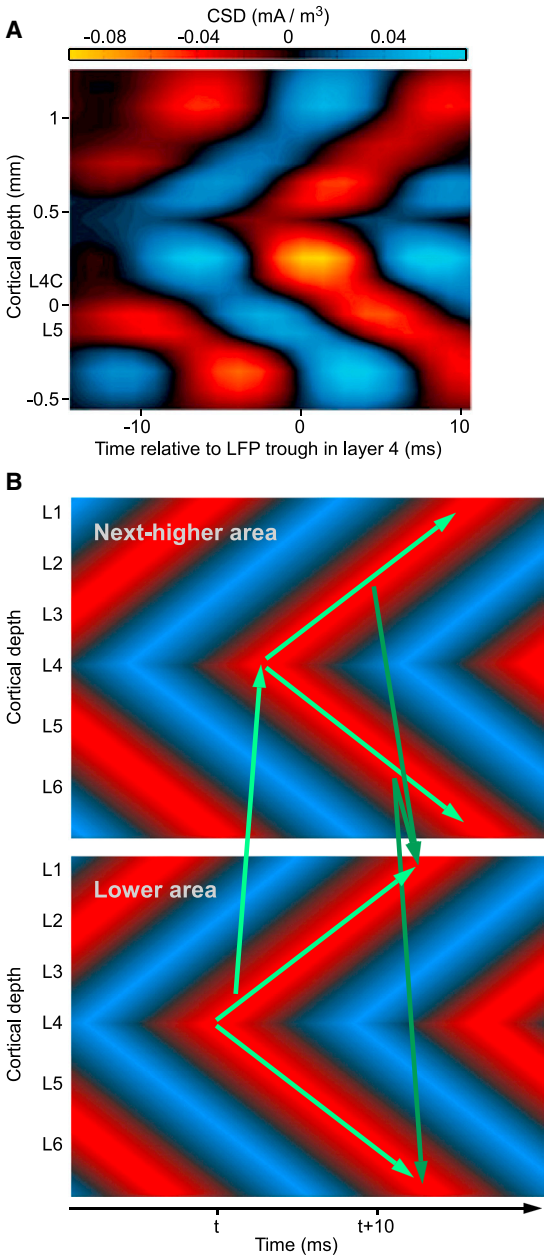

Figure 3. Interlaminar Delays Might Compensate for Interareal Feedforward and Feedback Delays

(A) Analysis of current source density (CSD) derived from laminar recordings in awake monkey area V1 (adapted and modified from van Kerkoerle et al., 2014). Laminar CSD was averaged relative to troughs in the gamma-filtered LFP from layer 4. The analysis reveals interlaminar gamma-band synchronization with systematic delays as a function of distance from layer 4.

(B) The interlaminar delays might delay the supra- and infragranular gamma phase such that reentrant feedback arrives at the excitable phase of the same, delayed, gamma cycle (Bastos et al., 2015b). Cortical depth is indicated by approximate position of the different cortical layers, abbreviated as L1–L6. Arrows indicate the proposed flow of gamma-mediated signaling. Interareal arrows conform to the known laminar pattern of feedforward and feedback connections (Markov et al., 2014). Note that the CSD analyses do not reflect the finding that gamma-band spike-LFP coherence is stronger in superficial as compared to deep layers (Buffalo et al., 2011).

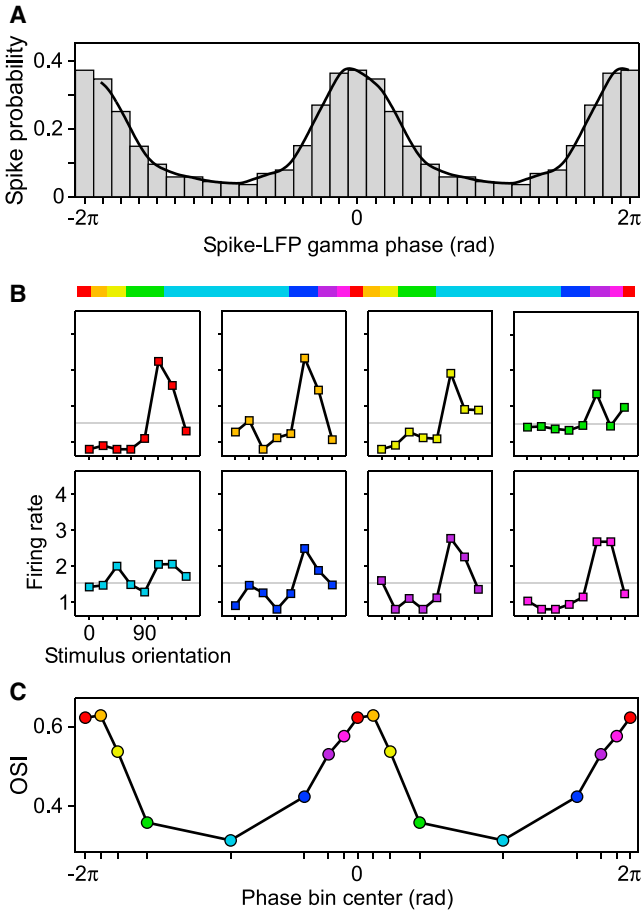

Figure 4. The Gamma Cycle Implements Pulsatile Neuronal Representations

(A–C) Awake monkey V1 single unit during visual stimulation with a drifting grating (adapted and modified from Womelsdorf et al., 2012).

(A) Spike probability as function of the gamma phase in LFPs, which were recorded simultaneously from separate nearby electrodes.

(B) The colored bar shows the partitioning of the gamma cycle into eight phase bins containing equal numbers of spikes (aligned to the phase in the gamma cycle to which spikes synchronized on average). Orientation tuning curves calculated separately for the eight gamma phase bins show a strong modulation of orientation selectivity with gamma phase, even though spike count was equal.

(C) Orientation selectivity index (OSI) as function of the gamma phase bin, in which the spikes occurred.

Gamma-Band Coherence Renders Communication Selective

In addition to rendering communication effective and precise, coherence also renders communication selective. If one set of synaptic inputs, constituting one neuronal representation, succeeds in triggering postsynaptic excitation followed by inhibition, this inhibition closes the door in front of other inputs. Those other inputs are then unable to transmit the neuronal representation that they constitute, and they are unable to trigger inhibition themselves. Thereby, the winning set of synaptic inputs conquers the perisomatic inhibition in the postsynaptic neuronal group, entrains it to its own rhythm, and thereby establishes a communication link that is selective or,

in other words, exclusive (Börgers and Kopell, 2008; Gielen et al., 2010).

CTC Implements Attentional Selection

This selective communication link is an ideal candidate mechanism for implementing selective attention, concretely the selective routing of attended sensory representations. When, e.g., one out of several visual stimuli is attended, because it is behaviorally relevant, the early visual cortical representation of this attended stimulus is preferentially communicated to postsynaptic neuronal groups, at the expense of other, unattended, stimuli (Reynolds et al., 1999). From lower to higher areas of visual cortex, neuronal projections converge such that postsynaptic neurons respond selectively to particular conjunctions of simpler stimulus features; at the same time, this convergence renders responses invariant, i.e., insensitive to stimulus dimensions like the precise stimulus position, which are already represented with high precision in early visual areas (Ito et al., 1995). This increasing spatial invariance with increasing hierarchical level is reflected in increasing receptive field (RF) sizes. Invariance appears necessary, because it readily offers a neuronal mechanism of stimulus recognition unperturbed by stimulus deviations in irrelevant details. Also, it avoids a combinatorial explosion that would result, if object-selective higher-area neurons represented particular sensory realizations of particular object tokens. Yet, the convergence that produces both stimulus selectivity and invariance unavoidably results in a situation in which a given postsynaptic neuron often receives synaptic inputs containing the representations of more than one perceptual object (Fries, 2009). When a single neuron in a higher visual area responds with different firing rates to different stimuli, the simultaneous presentation of both stimuli in the neuron's RF results in a firing rate that is a weighted average of the response to the isolated stimuli (Reynolds et al., 1999). This is the case when attention is directed away from both stimuli. However, when attention is directed toward one of the two stimuli, the firing rate of the postsynaptic neuron represents primarily the attended stimulus (Reynolds et al., 1999; Zhang et al., 2011). In the same attention tasks, presynaptic neurons in lower visual areas, whose smaller RFs contain only one of the two stimuli, show only small effects of attention on their firing rates (Luck et al., 1997). Thus, with two visual stimuli, there are two sets of presynaptic neurons in lower visual areas, with firing rates hardly affected by attention, and postsynaptic neurons in higher visual areas, with firing rates dominated by the attended stimulus. This can be modeled elegantly if attention modulates the effective strength of the synaptic inputs from lower visual neurons onto higher visual neurons, i.e., the synaptic gain, and the respective models are explicitly ignorant about the mechanism of gain modulation (Reynolds et al., 1999; Reynolds and Heeger, 2009). I suggest that CTC is an ideal mechanism to implement the attentional modulation of input gain. As the term "input gain" conveys, the attentional modulation acts on the sets of synaptic inputs signaling the competing stimuli. At the postsynaptic neuron, those sets of synaptic inputs are likely distributed over the dendritic tree and partly intermingled. If attention were to act somehow directly on those synapses, e.g., through anatomical top-down projections ending in synapses onto those synapses, this would require intricate addressing of the synapses conveying the attended stimulus. By contrast, in the CTC scenario, attentional top-down control does not address the synapses signaling the attended stimulus, but rather it simply addresses the corresponding neurons in the lower area. The rhythmic synchronization of those neurons manages to entrain postsynaptic neurons and thereby achieves the increase in input gain at the postsynaptic neurons.

This central prediction of the CTC hypothesis has recently received direct support from two independent yet very similar experimental studies (Bosman et al., 2012; Grothe et al., 2012). We illustrate here one of the studies (Figure 5) (Bosman et al., 2012). Macaque monkeys fixated while two stimuli, positioned next to each other at the same eccentricity a few degrees away from fixation, were presented either separately (Figures 5A–5D) or simultaneously (Figures 5E–5H). During simultaneous presentations, one of the stimuli was behaviorally relevant, the other was irrelevant, and the monkey's behavior indicated that the relevant stimulus was attended and the irrelevant one ignored. Neuronal recordings were performed simultaneously in the lower visual area V1 and the higher visual area V4. The two stimuli activated two separate groups of neurons in V1 (Figure 5B), and there were neuronal groups in V4 that were activated by either stimulus to approximately the same degree (Figure 5D). When one of the stimuli was presented separately, it induced a gamma rhythm in its respective V1 neuronal group, which entrained the V4 neuronal group (Figure 5C). When both stimuli were presented simultaneously, both stimuli induced a gamma rhythm in their respective V1 neuronal group (Figure 5F). Crucially, when one of the two simultaneously presented stimuli was attended, only the corresponding V1 gamma managed to entrain the V4 gamma (Figure 5G). The ignored stimulus induced a gamma rhythm in V1, which did however fail to entrain the V4 gamma. The CTC hypothesis suggests that this selective entrainment of V4 gamma by the attended V1 gamma is the cause for the selective routing of the attended stimulus from V1 to V4. This proposal is also supported by corresponding mathematical models (Börgers and Kopell, 2008; Gielen et al., 2010).

These results raise important questions for further investigation. In particular, we will need to understand better how attentional top-down influences result in the selective interareal synchronization. In the CTC scenario, attentional top-down influences do not need to address the synapses to postsynaptic neurons in a higher area, where the competing stimuli are difficult to disentangle. Rather, attentional top-down influences can be addressed to the presynaptic neurons in a lower area, which are arranged in maps, with neurons of similar preferences located close to each other. Attentional top-down control can therefore address neurons belonging to the neuronal representation of a given stimulus often by simply addressing a spatially coherent neuronal group. This holds most straightforwardly for spatially specific attention. I would like to speculate that top-down influences implementing attention to nonspatial stimulus features similarly address neurons in areas, where those stimulus features are represented in topographically ordered and thereby easily addressable maps. Top-down influences among neighboring areas might be refined by the above-discussed mechanism that renders feedback from the receiving group more effective at the coherent sending group than at the

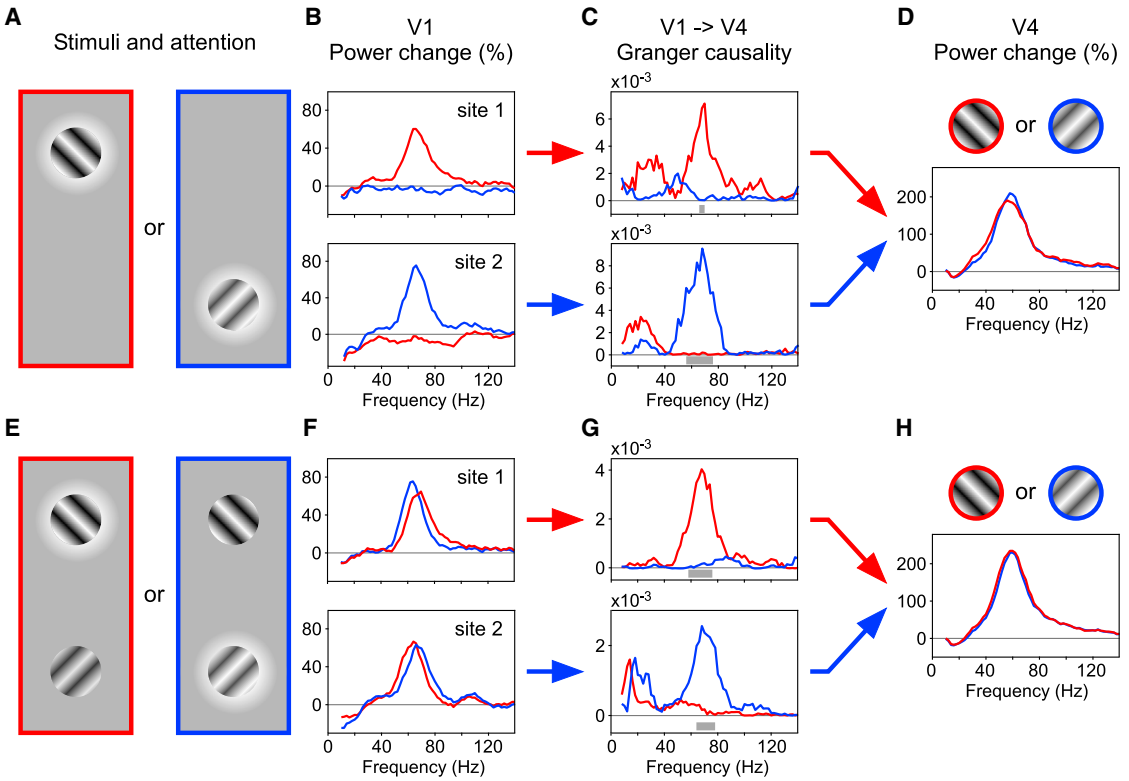

Figure 5. Selective Attention through Selective Interareal Granger-Causal Influences in the Gamma Band

Triplet recording of two sites in V1 (B and F) and one site in V4 (D and H), allowing the analysis of Granger-causal (GC) interareal influences (C and G) (adapted and modified from Bosman et al., 2012).

(A–D) Two conditions with a single visual stimulus each, showing the stimulus selectivity of the recorded neuronal signals.

(A) Illustration of the two conditions. The stimuli were behaviorally relevant and therefore attended, as indicated by their halo. Red and blue frames are not shown to the monkey, but are used to label the corresponding spectra in the following panels.

(B) Spectral power changes, relative to pre-stimulus baseline, for the two V1 sites. Each site showed visually induced gamma-band activity exclusively for one of the two stimuli.

(C) GC influence spectra, showing the feedforward influences of V1 onto V4.

(D) Spectral power change, relative to prestimulus baseline, for the V4 site. The site showed visually induced gamma-band activity that was very similar for the two stimuli.

(E–H) Same as (A)–(D), but for two conditions with two visual stimuli and selective attention to one of them. (F) In V1, selective attention enhances gamma peak frequency (see also Figures 6A and 6B). (G) V1 exerts feedforward influence onto V4 almost exclusively through the gamma rhythm induced by the attended stimulus. (H) V4 responds equally strongly to both conditions. Previous studies have demonstrated that spike rates of single neurons in V4 predominantly represent the attended stimulus (Moran and Desimone, 1985; Reynolds et al., 1999), as indicated by the stimulus symbols above the panel.

noncoherent sending group, even if it is anatomically directed to both (Bastos et al., 2015b; Fries, 2005).

This still leaves open the question of how the top-down addressed neuronal groups are brought into selective synchronization with the postsynaptic neurons in higher visual areas. A parsimonious assumption is that attentional top-down influences modify gamma-band synchronization in the lower-area neuronal group in such a way that it has a competitive advantage in entraining the postsynaptic neuronal group (Lee et al., 2013). This might be achieved by modulation in gamma-band synchronization strength or frequency, and I will discuss evidence for both in the following two paragraphs.

Selective Attention Modulates Gamma-Band Synchronization Strength

The first option is that attentional top-down influence affects the strength of gamma-band synchronization in the lower area. Importantly, in this context, the lower area is simply the area with RFs small enough to contain only one of the multiple stimuli, because then the competition occurs at the input to the next higher area. For example, two closely spaced stimuli might fall into separate V1 RFs and compete inside the same V4 RF, whereas two more separated stimuli might fall into different V4 RFs and compete inside the same RF in the subsequent area TEO.

When two stimuli are separated such that a local group of V4 neurons is activated by only one of them, selective attention to that stimulus results in enhanced gamma-band synchronization among the V4 neurons (Bichot et al., 2005; Fries et al., 2001), which is predictive of shortened reaction times on a trial-by-trial basis (Womelsdorf et al., 2006). This holds at least if gamma-band synchronization is assessed by means of LFP power (Taylor et al., 2005) or the coherence between multiunit activity (MUA) (Fries et al., 2008). Yet, when MUA, showing an attentional enhancement of gamma-band synchronization, is broken down into single units, a differential effect of attention is revealed

(Vinck et al., 2013): attention decreases the gamma locking of the less active or less stimulus-activated neurons, whereas it increases the gamma locking of the more active or more stimulus-activated neurons. This increased gamma-band synchronization among the most active units likely endows them with a larger influence onto postsynaptic neurons (Azouz and Gray, 2003; Salinas and Sejnowski, 2001). It could thus be a mechanism through which attentional top-down mechanisms lend the lower-area neurons representing the attended stimulus a competitive advantage in entraining postsynaptic neurons in higher areas.

An interesting question is whether similar effects of attentional top-down influences occur in primary visual cortex, V1. When gamma-band synchronization in V1 is assessed as LFP power or as spike-LFP coherence without differentiating between more versus less active/activated neurons, inconsistent results have been reported: different studies found decreases (Chalk et al., 2010), an absence of a change (Bosman et al., 2012), and increases (Buffalo et al., 2011; van Kerkoerle et al., 2014). The overall weaker effect of attention on gamma-band synchronization in V1 as compared to V4 might be due to (1) weaker attentional influences, or (2) more pronounced stimulus selectivity potentially leading to an attentional decrease of gamma synchronization for a large majority and an increase only for a small minority of single neurons. Because in V4 attention leads to both gamma-synchronization increases (for strongly active/activated neurons) and decreases (for weakly active/activated neurons), it is possible that similar effects occur in V1 and explain the diverse findings there so far.

Selective Attention and Stimulus Salience Modulate Gamma-Band Synchronization Frequency

An additional mechanism that might lend a neuronal group a competitive advantage in entraining postsynaptic neurons is an enhanced gamma-band synchronization frequency. When two simulated oscillators with slightly different intrinsic frequencies are reciprocally coupled, they can synchronize fully or partially. During periods of synchronization, the oscillator with the higher intrinsic frequency leads over the one with the lower intrinsic frequency (Cannon et al., 2014; Lowet et al., 2015) and thereby exerts a relatively stronger influence. Correspondingly, when two V1 gamma rhythms compete for entraining V4 gamma, it is conceivable that the faster V1 gamma rhythm exerts a stronger influence on V4, simply by means of its higher frequency (Cannon et al., 2014).

The abovementioned recordings in monkey visual cortex (Bosman et al., 2012) indeed revealed that selective attention leads to a consistent increase in the V1 gamma peak frequency by about 3 Hz (Figures 6A and 6B). Intriguingly, gamma peak frequency systematically increases also with increasing stimulus contrast (Figure 6D) (Hadjipapas et al., 2015; Jia et al., 2013b; Lowet et al., 2015; Ray and Maunsell, 2010; Roberts et al., 2013). Stimulus contrast and selective attention have closely related effects on neuronal processing (Reynolds and Chelazzi, 2004; Reynolds and Heeger, 2009), with attention increasing the effective contrast of an attended stimulus by about 50% (Reynolds et al., 2000). If stimulus contrast invoked the same gamma-frequency-enhancing mechanisms as selective attention, a 50% contrast enhancement should result in a 3 Hz gamma-frequency increase. This corresponds well to the finding that a 50% contrast increase leads to a 4 Hz gamma-frequency increase (Ray and Maunsell, 2010) (the study reported a linear fit between the gamma frequency and $\log_2$ [contrast] with a slope of 6.8 Hz).

Interestingly, gamma peak frequency also systematically increases with other stimulus properties that increase stimulus strength and salience, namely with the elimination of superimposed noise (Figure 6E) (Jia et al., 2013b), with stimulus motion (Figure 6G) (Friedman-Hill et al., 2000; Gray et al., 1990; Muthukumaraswamy and Singh, 2013; Swettenham et al., 2009; van Pelt and Fries, 2013), and with a stimulus location closer to the fovea (Figure 6H) (Lima et al., 2010; van Pelt and Fries, 2013). Also, stimulus onsets lead to higher gamma peak frequency (Figure 6C), a phenomenon illustrated in many studies even though not often reported explicitly (Fries et al., 2001; Hoogenboom et al., 2006). In addition, gamma peak frequency increases also with decreasing stimulus size (Figure 6F) (Gieselmann and Thiele, 2008; Jia et al., 2013b; Ray and Maunsell, 2011). The relation of stimulus size to stimulus salience is less clear. Yet, one might speculate that larger stimuli might increasingly be treated as nonsalient background. Gamma peak frequency increases are not simply due to higher firing rates. When the salience of drifting gratings is reduced by superimposing dynamic noise, this is reflected in reduced gamma peak frequency (Figure 6E), but not in firing rate changes (Jia et al., 2013b). Similarly, when stimulus orientation is varied around the neuron's preferred orientation, this by definition changes firing rates, but it does not change stimulus salience, and correspondingly, it also does not systematically affect gamma frequency (Figure 6I) (Friedman-Hill et al., 2000; Gray et al., 1990; Jia et al., 2013b). At any given moment, gamma frequency is likely influenced by several factors simultaneously. The described effects of stimulus salience and attention likely interact with each other and with further effects. For example, gamma frequency also increases with stimulus repetition (Brunet et al., 2014).

I would like to speculate that the competitive advantage of the faster V1 gamma is potentiated by a regular reset of gamma phase by a theta rhythm, as has been found in awake monkey visual cortex (Bosman et al., 2009). For the first few gamma cycles after the reset, the faster gamma rhythm sends its inputs to V4 a few milliseconds before competing slower gamma rhythms (Figure 7). The earlier arrival of input from the faster gamma allows these inputs to trigger inhibition of the postsynaptic network and thereby to shut out competing inputs mediated by slower gamma rhythms. In essence, stimulus salience and top-down attention are translated into gamma frequency, and theta-rhythmic gamma phase resets turn V1 gamma-frequency differences into V4 input-latency differences, with the earliest input representing the most salient and/or attended stimulus (Bosman et al., 2012). After a few gamma cycles, once V4 is entrained by the winning V1 rhythm, the interareal locking might sustain the selection for the remainder of the theta cycle, even when the two gamma rhythms precess against each other and thereby produce arbitrary lead-lag relationships. The stability of an established gamma-band entrainment against precession has been suggested by mathematical models (Börgers and Kopell, 2008).

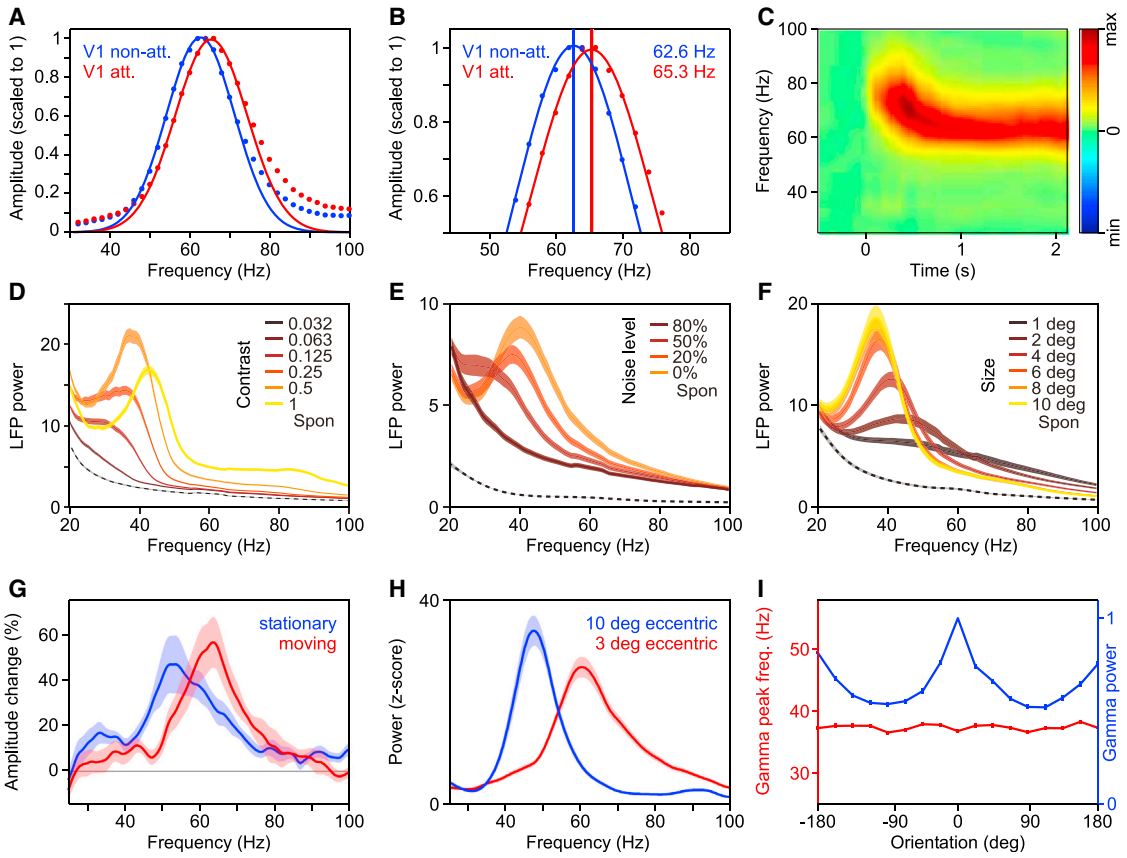

Figure 6. The Gamma-Band Peak Frequency Increases with Attention and Salience

(A and B) Dots show awake macaque V1 LFP power changes (scaled to peak at a value of one) induced by a grating stimulus, when it was nonattended (blue) or attended (red), lines show Gaussian fits (adapted and modified from Bosman et al., 2012). (B) shows a detail of (A) at higher resolution.

(C) Human MEG power change over early visual cortex as a function of time after stimulus onset. Note that the gamma peak frequency is higher at response onset than during the sustained response (adapted and modified from van Pelt et al., 2012).

(D–F) Anesthetized macaque V1 LFP power, during visual stimulation with a grating of varying contrast (D), varying amount of superimposed noise (E), and varying size (F), as indicated by inset color legends (adapted and modified from Jia et al., 2013b).

(G) Human MEG power change, estimated to emerge from primary visual cortex, during visual stimulation with a grating that is stationary (blue) or moving (red) (adapted and modified from Swettenham et al., 2009).

(H) Awake macaque V1 LFP power during stimulation with a large grating that activated a recording site with a peripheral RF (blue) and another recording site with a foveal RF (red) (adapted and modified from Lima et al., 2010).

(I) Anesthetized macaque V1 LFP gamma peak frequency (red line and left y axis) as well as gamma power (blue line and right y axis) as a function of stimulus orientation relative to the recording site's preferred orientation (adapted and modified from Jia et al., 2013b).

Stimulus salience, e.g., due to contrast or motion, is often within a narrow range within a given visual object, yet changes at object boundaries (Lowet et al., 2015). Moreover, visual attention during natural viewing operates at the level of objects (Nuthmann and Henderson, 2010). Thereby salience- and attention-dependent gamma frequency changes likely contribute to synchronization of neurons activated by one object and desynchronization of neurons driven by different objects (Lowet et al., 2015). Crucially, across the hierarchy of visual areas, neuronal groups activated by the same visual stimulus naturally see the same stimulus salience and attention and thereby have the same gamma frequency. Where projections to higher areas converge, the higher gamma frequency likely succeeds in selectively entraining postsynaptic neurons.

Thus, both the frequency and the strength of gamma-band synchronization might lend a competitive advantage to the lower-area neuronal group that is activated by the attended stimulus in entraining postsynaptic neurons in higher areas. The selective entrainment of the higher area to the part of the lower area representing the attended stimulus constitutes the implementation of attentional selection. It is important to make the distinction between the implementation of attentional selection and the control of attentional selection. While the control of attentional selection is exerted by frontal and parietal areas through top-down influences onto visual areas, the implementation of attentional selection is realized by selective bottom-up influences of lower onto higher visual areas. Therefore, as much as it makes sense that the implementation is through selective interareal gamma-band synchronization, which is predominantly bottom-up, the control is expected to be through top-down influences of frontoparietal areas onto visual areas and/or higher visual areas onto

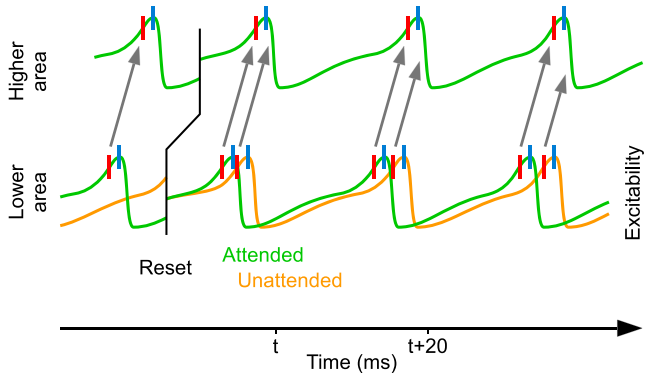

Figure 7. Theta-Rhythmic Phase Reset Turns Gamma-Frequency Differences into Latency Differences

In the lower area, after a reset, the gamma rhythms representing different stimuli start at the same phase. The gamma rhythm representing the attended stimulus (green) is faster than the gamma rhythm representing the unattended stimulus (orange). This frequency difference translates into a latency difference. The input from the attended representation reaches the higher area first, transmits its representation, and triggers inhibition to shut out the competing unattended representation.

lower visual areas (Buffalo et al., 2010; Buschman and Miller, 2007).

Top-Down Influences Are Mediated by Alpha-Beta-Band Rhythms

A recent study has investigated the top-down-directed influences among eight primate visual areas, including parietal and frontal visual control areas. In the gamma band, bottom-up influences were stronger than top-down influences, yet the opposite was the case for the beta band, in which top-down influences were stronger than bottom-up influences (Figure 8A) (Bastos et al., 2015a). This pattern of directed interareal influences agrees well with another finding, namely that in primate visual areas V1, V2, and V4, gamma-band synchronization is particularly strong in superficial cortical layers, whereas alpha/beta-band synchronization is particularly strong in deep cortical layers (Figure 8C) (Buffalo et al., 2011). Superficial cortical layers are the primary source of anatomical forward projections, and this predominance increases with the number of hierarchical levels that are bridged by the forward projections; deep cortical layers are the primary source of anatomical backward projections, and this predominance increases with the number of hierarchical levels that are bridged by the backward projections (Markov et al., 2014). Thus, the degree to which an anatomical projection originates from superficial layers, measured by the supragranular labeled neuron proportion after retrograde tracing (SLN), quantifies the degree to which a projection is of a feedforward type (Barone et al., 2000). Consistent with the laminar differences in gamma- versus beta-band synchronization, the anatomical SLN metric correlates with the asymmetry in directed influences (Figure 8B) (Bastos et al., 2015a). These data suggest that supragranular layers convey their signals through the gamma rhythm, whereas infragranular layers use the beta rhythm. Note that weak top-down projections can originate in supragranular layers and weak bottom-up projections in infragranular layers, for areas close to each other in the hierarchy (Markov et al., 2014). Correspondingly, for those neighboring areas, there are also weak top-down gamma influences and weak bottom-up beta influences (Bastos et al., 2015a).

A similar dissociation with higher frequencies mediating feedforward and lower frequencies mediating feedback signals has also been found outside visual cortex. One study investigated Granger causality between lower and higher auditory cortex of human patients with implanted electrodes and reported feedforward signaling in gamma and feedback signaling in delta to beta bands (Fontolan et al., 2014). Yet, outside visual cortex also counterexamples have been reported for parietal-auditory and parietal-somatosensory influences (Brovelli et al., 2004; Roopun et al., 2010).

Among visual areas, the notion that gamma mediates forward and beta mediates backward influences received further support from a study using electrical stimulation in either V1 or V4 and LFP recordings in the respective other area (van Kerkoerle et al., 2014). When electrical stimulation (five pulses at 200 Hz) was given to V1, this robustly induced enhanced gamma-band LFP power in V4, consistent with a forward influence (Figure 8D); when the same electrical stimulation was given to V4, then under visual stimulation with a background stimulus, this induced enhanced alpha-band LFP power in V1 (Figure 8E). The frequencies related to top-down influences differ across the studies between alpha and beta, and the precise reason or relative role of the two neighboring bands is not yet clear.

These results predict that top-down beta-band influences should be enhanced when a cognitive task requires stronger top-down control. A task modulating top-down control is selective attention, in which both bottom-up stimulation and task difficulty are constant, and top-down influences should be specifically enhanced toward the visual cortex representing the attended stimulus. Indeed, top-down beta-band influences among visual areas contralateral to the attended stimulus were found to be larger than among ipsilateral areas (Bastos et al., 2015a). This is consistent with a study reporting that attention enhances 8–15 Hz coherence between areas V4 and TEO and between those areas and the Pulvinar (Saalmann et al., 2012). Enhanced top-down beta-band influences might lead to enhanced bottom-up gamma-band influences (Bosman et al., 2012; Grothe et al., 2012), and a recent modeling study suggests a putative mechanism (Lee et al., 2013). Also during other tasks, conditions expected to strengthen feedback influences resulted in stronger synchronization in relatively lower frequency bands (Arnal et al., 2011; Buschman and Miller, 2007; Kornblith et al., 2015; von Stein et al., 2000).

Theta-Rhythmic Gamma-Band Synchronization Implements Attentional Sampling

The experimental evidence presented and the considerations discussed so far suggest that top-down attentional influences are mediated by beta-band synchronization, that the selective communication of the attended stimulus is implemented by gamma-band synchronization, and that gamma is rhythmically reset by a 4 Hz theta rhythm. The theta-rhythmic resetting entails a modulation of gamma-synchronization strength, consistent with several studies reporting gamma-strength modulation with theta phase (Figure 9A) (Bosman et al., 2009, 2012; Bragin

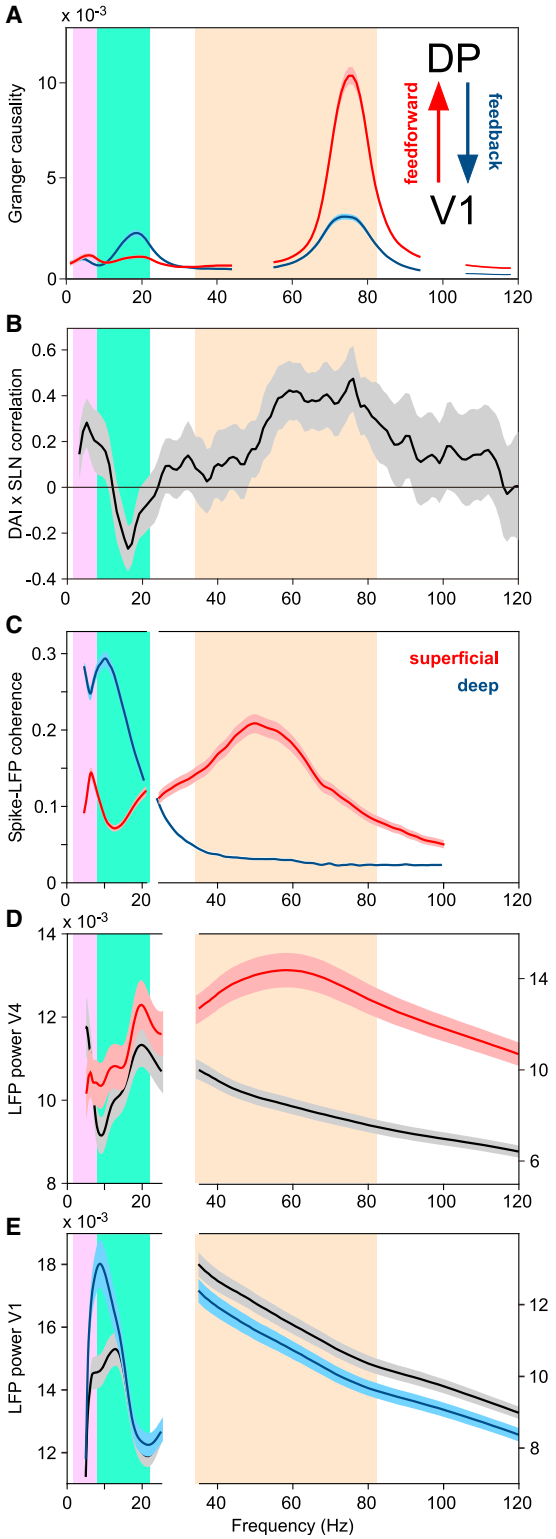

Figure 8. Feedforward Predominates in Theta and Gamma Bands, Feedback in the Alpha-Beta Band

(A) Granger-causal influences between awake macaque areas V1 and DP. The influence in the V1-to-DP direction is through an anatomical feedforward-type projection and predominates in the theta and gamma bands, indicated by purple and orange backgrounds, respectively. The influence in the DP-to-V1 direction is through an anatomical feedback-type projection and predominates in the beta band, indicated by green background.

(B) The Spearman-rank correlation, across area pairs, between an anatomical metric of the feedforward/feedback character of an interareal projection (SLN) and an electrophysiological metric of the asymmetry in Granger-causal influences (DAI). A positive (negative) correlation value indicates that Granger-causal influences in the respective frequency are stronger in the anatomically defined feedforward (feedback) direction. (A) and (B) are adapted and modified from Bastos et al. (2015a).

(C) Spike-LFP coherence from awake macaque area V2, for recordings from deep (blue) and superficial (red) layers. Spike-LFP coherence shows an alpha-beta band peak for deep layers and both a theta and a gamma peak for superficial layers (adapted and modified from Buffalo et al., 2011).

(D) Awake macaque V4 LFP power during visual stimulation with a background stimulus (black) and additional electrical stimulation in V1 (five pulses at 200 Hz), which leads to power enhancement in the gamma band (red).

(E) Awake macaque V1 LFP power during visual stimulation with a background stimulus (black) and additional electrical stimulation in V4 (five pulses at 200 Hz), which leads to power enhancement in the alpha-beta band (blue). (D) and (E) are adapted and modified from van Kerkoerle et al. (2014).

et al., 1995; Canolty et al., 2006; Colgin et al., 2009; Schomburg et al., 2014; Voloh et al., 2015). If we identify a gamma-synchronized network with the attentional selection of the respective stimulus, then the theta-rhythmic gamma resetting corresponds to the termination of this attentional selection and a potential shift of attention to another stimulus. Attentional shifts are expressed overtly during natural viewing as gaze shifts, i.e., saccades. Strikingly, saccades during natural viewing show intersaccadic interval distributions with a strong Gaussian component at 145 ms (Figures 9B and 9C), consistent with a 7 Hz theta rhythm (Otero-Millan et al., 2008).

Together, these data suggest that the theta rhythm constitutes a visual (and maybe a general) exploration routine (Fries, 2009). When the behavioral context allows the eyes to explore the visual environment freely, they saccade at a theta rhythm. When the context requires the eyes to fixate for prolonged durations, the cortical theta phase modulates the strength of gamma-band synchronization (Bosman et al., 2009), which we identified as implementation of attentional selection. Thus, it is conceivable that irrespective of saccades as overt expressions of attention, selective attention samples visual input at a theta rhythm.

A recent study lends direct support to this (Landau and Fries, 2012). Human subjects were required to fixate and report a contrast decrement occurring at a random time per trial in one of two gratings positioned in the right and left visual hemifield. A task-irrelevant flash occurred around one of the gratings at a random time relative to the to-be-detected contrast decrement and shifted attention to the respective grating. This attentional reset to one side was particularly successful when the flash occurred in the right visual field. After right visual field flashes, 4 Hz theta rhythms were directly visible in the time courses of behavioral performance at both stimulus locations, and the two rhythms were in antiphase (Figures 9D and 9E). Another study used a similar approach to investigate detection performance at uncued locations, at which changes occurred with 25% probability, and which were either on the same or a different object as the cued location, at which changes occurred with 75% probability (Fiebelkorn et al., 2013). This revealed attentional sampling of the uncued locations at 4 Hz and in antiphase. Yet

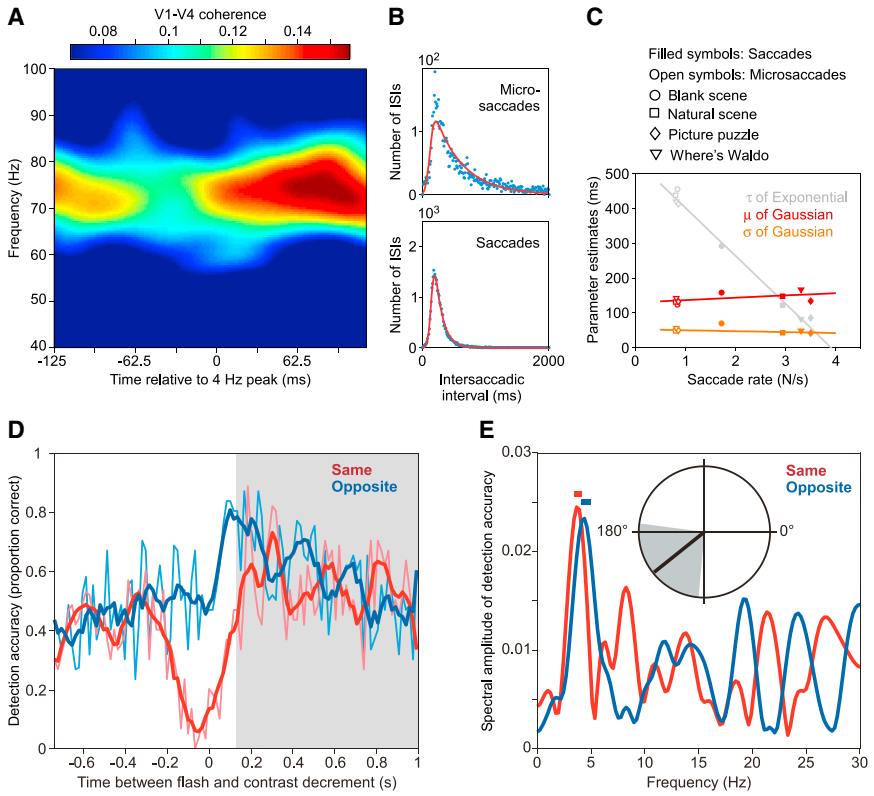

Figure 9. A Theta Rhythm Is Visible in Visual Gamma, Saccades, and Attentional Sampling

(A) V1–V4 coherence as a function of frequency and of time in the 4 Hz theta cycle (adapted and modified from Bosman et al., 2012).

(B) Histograms of intersaccadic intervals (ISIs) for microsaccades and regular saccades during free viewing of natural scenes.

(C) The histograms of (B) have been fitted with ex-Gaussian functions. The resulting parameter estimates are shown for microsaccades and saccades observed during several viewing conditions as indicated. Irrespective of condition, the Gaussian component's mean was around 145 ms, corresponding to 7 Hz. (B) and (C) are adapted and modified from Otero-Millan et al. (2008).

(D) Detection accuracy for equally probable contrast decrements on two bilateral stimuli, after an irrelevant flash at time zero.

(E) Spectral analysis of the time-resolved detection accuracy from (D). The amplitude spectra reveal peaks close to 4 Hz. The 4 Hz phase relation of detection accuracy contralateral versus ipsilateral to the flash is shown in the inset, has a mean of 222°, and is not significantly different from 180°. (D and E) are adapted and modified from Landau and Fries (2012).

another very recent study demonstrated that the 4 Hz sampling of two simultaneously attended stimuli does not only occur after a reset event, but that it is present continuously during distributed attention (Landau et al., 2015). Subjects monitored two equally relevant stimuli for an unpredictable small change, and the gamma-band activities induced by the two stimuli were subtracted from each other to reveal moment-by-moment attentional biases to one or the other stimulus. The 4 Hz phase of this gamma difference preceding the stimulus change predicted whether subjects were better or worse in detecting the change. This suggests that the gamma-band activities induced by the two stimuli are enhanced at 4 Hz in alternation, whenever the respective stimulus is attentionally sampled.

These results can be parsimoniously explained by an 8 Hz attentional sampling process. If this process samples two stimuli, each stimulus is sampled four times per second, i.e., at a 4 Hz rhythm. This would predict that a single object would be sampled at around 8 Hz and, e.g., three stimuli at around 8/3 = 2.7 Hz. Indeed, detection performance of a single location fluctuates and can be partly predicted by the prestimulus phase of the ongoing 7.1 Hz component of frontal EEG (Busch et al., 2009). An elegant psychophysical study investigated human tracking performance on one, two, and three moving targets while varying temporal frequency of the tracked stimuli. This revealed that temporal frequency limits fell from 7 Hz with one target to 4 Hz with two targets and 2.6 Hz with three targets (Holcombe and Chen, 2013). These results are consistent with a 7–8 Hz sampling process that is divided over one, two, or three stimuli.

Conclusions

Based on the synopsis of the presented evidence and considerations, I would like to suggest the following scenario: Local cortical neuronal groups synchronize by default in the alpha band. During alpha-band synchronization, network excitation fluctuates at 100 ms cycles, but is tracked by network inhibition within 3 ms. This curtails effective communication and renders the respective activity invisible to other neurons. It allows holding "on-stock" local neuronal representation, which can be accessed flexibly. It might be an important contribution to making optimal use of the brain's massively parallel processing architecture. Attention samples from this internal store at a theta rhythm. Attentional top-down influences are mediated by alpha-beta-band synchronization. It is possible that top-down influences in alpha and beta bands have differential roles. Top-down alpha influences might convey influences that reinforce local alpha, e.g., for irrelevant background regions. Top-down beta influences wake up the local circuit and modulate its gamma-band synchronization by strengthening it among the most stimulus-driven neurons, and by enhancing its frequency. Visual scenes induce many local gamma rhythms with varying strength and frequency, reflecting the bottom-up stimulus salience and stimulus history. The resulting gamma landscape in, e.g., V1 thus reflects stimulus properties, experience, and top-down influences. At a given time point, one out of these co-existing gamma rhythms succeeds in entraining postsynaptic neuronal groups. This gamma entrainment allows to transmit a stimulus representation and to selfishly shut out competing stimuli's representations. The entrainment establishes a cycle-to-cycle memory of the active link that maintains until it is terminated at the end of a theta cycle. The presynaptic gamma rhythm allows network excitation to escape its ever-chasing network

inhibition. Inhibition is temporally focused, which allows excitation in between inhibition, and which synchronizes excitatory output to optimally drive postsynaptic neurons. The rhythmically synchronous communication establishes a pulsatile computation. During each pulse, a spike-rate-based stimulus representation passes through the respective synapses to a postsynaptic neuron. The temporal focusing in the pulse increases the precision with which postsynaptic currents combine. Neurons driven by preferred stimuli spike slightly earlier in the pulse, with higher postsynaptic impact. Thus, several rhythms and their interplay render neuronal communication effective, precise, and selective.

ACKNOWLEDGMENTS

I thank the members of my lab for contributing to the development of CTC and its experimental tests. I thank Nancy Kopell, Ayelet Landau, Christopher Lewis, Eric Lowet, Eric Maris, Alina Peter, Michael Schmid, Wolf Singer, Julien Vezoli, Martin Vinck, and Thilo Womelsdorf for helpful comments on the manuscript. This work was supported by a European Young Investigator Award, HFSP (RGP0070/2003), Volkswagen Foundation (I/79876), European Union (HEALTH-F2-2008-200728 and HBP-604102), NIH (1U54MH091657), DFG (FOR 1847), and LOEWE (NeFF).

REFERENCES

Ainsworth, M., Lee, S., Cunningham, M.O., Traub, R.D., Kopell, N.J., and Whittington, M.A. (2012). Rates and rhythms: a synergistic view of frequency and temporal coding in neuronal networks. Neuron *75*, 572–583.

Akam, T.E., and Kullmann, D.M. (2012). Efficient "communication through coherence" requires oscillations structured to minimize interference between signals. PLoS Comput. Biol. *8*, e1002760.

Arnal, L.H., Wyart, V., and Giraud, A.L. (2011). Transitions in neural oscillations reflect prediction errors generated in audiovisual speech. Nat. Neurosci. *14*, 797–801.

Atallah, B.V., and Scanziani, M. (2009). Instantaneous modulation of gamma oscillation frequency by balancing excitation with inhibition. Neuron *62*, 566–577.

Azouz, R., and Gray, C.M. (2003). Adaptive coincidence detection and dynamic gain control in visual cortical neurons in vivo. Neuron *37*, 513–523.

Barone, P., Batardiere, A., Knoblauch, K., and Kennedy, H. (2000). Laminar distribution of neurons in extrastriate areas projecting to visual areas V1 and V4 correlates with the hierarchical rank and indicates the operation of a distance rule. J. Neurosci. *20*, 3263–3281.

Bastos, A.M., Vezoli, J., Bosman, C.A., Schoffelen, J.M., Oostenveld, R., Dowdall, J.R., De Weerd, P., Kennedy, H., and Fries, P. (2015a). Visual areas exert feedforward and feedback influences through distinct frequency channels. Neuron *85*, 390–401.

Bastos, A.M., Vezoli, J., and Fries, P. (2015b). Communication through coherence with inter-areal delays. Curr. Opin. Neurobiol. *31*, 173–180.

Bichot, N.P., Rossi, A.F., and Desimone, R. (2005). Parallel and serial neural mechanisms for visual search in macaque area V4. Science *308*, 529–534.

Börgers, C., and Kopell, N.J. (2008). Gamma oscillations and stimulus selection. Neural Comput. *20*, 383–414.

Bosman, C.A., Womelsdorf, T., Desimone, R., and Fries, P. (2009). A microsaccadic rhythm modulates gamma-band synchronization and behavior. J. Neurosci. *29*, 9471–9480.

Bosman, C.A., Schoffelen, J.M., Brunet, N., Oostenveld, R., Bastos, A.M., Womelsdorf, T., Rubehn, B., Stieglitz, T., De Weerd, P., and Fries, P. (2012). Attentional stimulus selection through selective synchronization between monkey visual areas. Neuron *75*, 875–888.

Bragin, A., Jandó, G., Nádasdy, Z., Hetke, J., Wise, K., and Buzsáki, G. (1995). Gamma (40-100 Hz) oscillation in the hippocampus of the behaving rat. J. Neurosci. *15*, 47–60.

Brovelli, A., Ding, M., Ledberg, A., Chen, Y., Nakamura, R., and Bressler, S.L. (2004). Beta oscillations in a large-scale sensorimotor cortical network: directional influences revealed by Granger causality. Proc. Natl. Acad. Sci. USA *101*, 9849–9854.

Brunet, N.M., Bosman, C.A., Vinck, M., Roberts, M., Oostenveld, R., Desimone, R., De Weerd, P., and Fries, P. (2014). Stimulus repetition modulates gamma-band synchronization in primate visual cortex. Proc. Natl. Acad. Sci. USA *111*, 3626–3631.

Brunet, N., Bosman, C.A., Roberts, M., Oostenveld, R., Womelsdorf, T., De Weerd, P., and Fries, P. (2015). Visual cortical gamma-band activity during free viewing of natural images. Cereb. Cortex *25*, 918–926.

Buffalo, E.A., Fries, P., Landman, R., Liang, H., and Desimone, R. (2010). A backward progression of attentional effects in the ventral stream. Proc. Natl. Acad. Sci. USA *107*, 361–365.

Buffalo, E.A., Fries, P., Landman, R., Buschman, T.J., and Desimone, R. (2011). Laminar differences in gamma and alpha coherence in the ventral stream. Proc. Natl. Acad. Sci. USA *108*, 11262–11267.

Busch, N.A., Dubois, J., and VanRullen, R. (2009). The phase of ongoing EEG oscillations predicts visual perception. J. Neurosci. *29*, 7869–7876.

Buschman, T.J., and Miller, E.K. (2007). Top-down versus bottom-up control of attention in the prefrontal and posterior parietal cortices. Science *315*, 1860–1862.

Buzsáki, G., and Wang, X.J. (2012). Mechanisms of gamma oscillations. Annu. Rev. Neurosci. *35*, 203–225.

Cannon, J., McCarthy, M.M., Lee, S., Lee, J., Börgers, C., Whittington, M.A., and Kopell, N. (2014). Neurosystems: brain rhythms and cognitive processing. Eur. J. Neurosci. *39*, 705–719.

Canolty, R.T., Edwards, E., Dalal, S.S., Soltani, M., Nagarajan, S.S., Kirsch, H.E., Berger, M.S., Barbaro, N.M., and Knight, R.T. (2006). High gamma power is phase-locked to theta oscillations in human neocortex. Science *313*, 1626–1628.

Cardin, J.A., Carlén, M., Meletis, K., Knoblich, U., Zhang, F., Deisseroth, K., Tsai, L.H., and Moore, C.I. (2009). Driving fast-spiking cells induces gamma rhythm and controls sensory responses. Nature *459*, 663–667.

Chalk, M., Herrero, J.L., Gieselmann, M.A., Delicato, L.S., Gotthardt, S., and Thiele, A. (2010). Attention reduces stimulus-driven gamma frequency oscillations and spike field coherence in V1. Neuron *66*, 114–125.

Colgin, L.L., Denninger, T., Fyhn, M., Hafting, T., Bonnevie, T., Jensen, O., Moser, M.B., and Moser, E.I. (2009). Frequency of gamma oscillations routes flow of information in the hippocampus. Nature *462*, 353–357.

Csicsvari, J., Jamieson, B., Wise, K.D., and Buzsáki, G. (2003). Mechanisms of gamma oscillations in the hippocampus of the behaving rat. Neuron *37*, 311–322.

Felleman, D.J., and Van Essen, D.C. (1991). Distributed hierarchical processing in the primate cerebral cortex. Cereb. Cortex *1*, 1–47.

Fiebelkorn, I.C., Saalmann, Y.B., and Kastner, S. (2013). Rhythmic sampling within and between objects despite sustained attention at a cued location. Curr. Biol. *23*, 2553–2558.

Fontolan, L., Morillon, B., Liegeois-Chauvel, C., and Giraud, A.L. (2014). The contribution of frequency-specific activity to hierarchical information processing in the human auditory cortex. Nat. Commun. *5*, 4694.

Friedman-Hill, S., Maldonado, P.E., and Gray, C.M. (2000). Dynamics of striate cortical activity in the alert macaque: I. Incidence and stimulus-dependence of gamma-band neuronal oscillations. Cereb. Cortex *10*, 1105–1116.

Fries, P. (2005). A mechanism for cognitive dynamics: neuronal communication through neuronal coherence. Trends Cogn. Sci. *9*, 474–480.

Fries, P. (2009). Neuronal gamma-band synchronization as a fundamental process in cortical computation. Annu. Rev. Neurosci. *32*, 209–224.

Fries, P., Reynolds, J.H., Rorie, A.E., and Desimone, R. (2001). Modulation of oscillatory neuronal synchronization by selective visual attention. Science *291*, 1560–1563.

Fries, P., Nikolić, D., and Singer, W. (2007). The gamma cycle. Trends Neurosci. *30*, 309–316.

Fries, P., Womelsdorf, T., Oostenveld, R., and Desimone, R. (2008). The effects of visual stimulation and selective visual attention on rhythmic neuronal synchronization in macaque area V4. J. Neurosci. *28*, 4823–4835.

Gielen, S., Krupa, M., and Zeitler, M. (2010). Gamma oscillations as a mechanism for selective information transmission. Biol. Cybern. *103*, 151–165.

Gieselmann, M.A., and Thiele, A. (2008). Comparison of spatial integration and surround suppression characteristics in spiking activity and the local field potential in macaque V1. Eur. J. Neurosci. *28*, 447–459.

Gray, C.M., König, P., Engel, A.K., and Singer, W. (1989). Oscillatory responses in cat visual cortex exhibit inter-columnar synchronization which reflects global stimulus properties. Nature *338*, 334–337.

Gray, C.M., Engel, A.K., König, P., and Singer, W. (1990). Stimulus-dependent neuronal oscillations in cat visual cortex: receptive field properties and feature dependence. Eur. J. Neurosci. *2*, 607–619.

Gregoriou, G.G., Gotts, S.J., Zhou, H., and Desimone, R. (2009). High-frequency, long-range coupling between prefrontal and visual cortex during attention. Science *324*, 1207–1210.

Grothe, I., Neitzel, S.D., Mandon, S., and Kreiter, A.K. (2012). Switching neuronal inputs by differential modulations of gamma-band phase-coherence. J. Neurosci. *32*, 16172–16180.

Hadjipapas, A., Lowet, E., Roberts, M.J., Peter, A., and De Weerd, P. (2015). Parametric variation of gamma frequency and power with luminance contrast: a comparative study of human MEG and monkey LFP and spike responses. Neuroimage *112*, 327–340.

Haider, B., Duque, A., Hasenstaub, A.R., and McCormick, D.A. (2006). Neocortical network activity in vivo is generated through a dynamic balance of excitation and inhibition. J. Neurosci. *26*, 4535–4545.

Hasenstaub, A., Shu, Y., Haider, B., Kraushaar, U., Duque, A., and McCormick, D.A. (2005). Inhibitory postsynaptic potentials carry synchronized frequency information in active cortical networks. Neuron *47*, 423–435.

Havenith, M.N., Yu, S., Biederlack, J., Chen, N.H., Singer, W., and Nikolić, D. (2011). Synchrony makes neurons fire in sequence, and stimulus properties determine who is ahead. J. Neurosci. *31*, 8570–8584.

Holcombe, A.O., and Chen, W.Y. (2013). Splitting attention reduces temporal resolution from 7 Hz for tracking one object to <3 Hz when tracking three. J. Vis. *13*, 12.

Hoogenboom, N., Schoffelen, J.M., Oostenveld, R., Parkes, L.M., and Fries, P. (2006). Localizing human visual gamma-band activity in frequency, time and space. Neuroimage *29*, 764–773.

Ito, M., Tamura, H., Fujita, I., and Tanaka, K. (1995). Size and position invariance of neuronal responses in monkey inferotemporal cortex. J. Neurophysiol. *73*, 218–226.

Jensen, O., and Mazaheri, A. (2010). Shaping functional architecture by oscillatory alpha activity: gating by inhibition. Front. Hum. Neurosci. *4*, 186.

Jia, X., Tanabe, S., and Kohn, A. (2013a). γ and the coordination of spiking activity in early visual cortex. Neuron *77*, 762–774.

Jia, X., Xing, D., and Kohn, A. (2013b). No consistent relationship between gamma power and peak frequency in macaque primary visual cortex. J. Neurosci. *33*, 17–25.

Kornblith, S., Buschman, T.J., and Miller, E.K. (2015). Stimulus load and oscillatory activity in higher cortex. Cereb. Cortex, bhv182.

Landau, A.N., and Fries, P. (2012). Attention samples stimuli rhythmically. Curr. Biol. *22*, 1000–1004.

Landau, A.N., Schreyer, H.M., van Pelt, S., and Fries, P. (2015). Distributed attention is implemented through theta-rhythmic gamma modulation. Curr. Biol. *25*, 2332–2337.

Lee, J.H., Whittington, M.A., and Kopell, N.J. (2013). Top-down beta rhythms support selective attention via interlaminar interaction: a model. PLoS Comput. Biol. *9*, e1003164.

Lima, B., Singer, W., Chen, N.H., and Neuenschwander, S. (2010). Synchronization dynamics in response to plaid stimuli in monkey V1. Cereb. Cortex *20*, 1556–1573.

Livingstone, M.S. (1996). Oscillatory firing and interneuronal correlations in squirrel monkey striate cortex. J. Neurophysiol. *75*, 2467–2485.

Lowet, E., Roberts, M., Hadjipapas, A., Peter, A., van der Eerden, J., and De Weerd, P. (2015). Input-dependent frequency modulation of cortical gamma oscillations shapes spatial synchronization and enables phase coding. PLoS Comput. Biol. *11*, e1004072.

Luck, S.J., Chelazzi, L., Hillyard, S.A., and Desimone, R. (1997). Neural mechanisms of spatial selective attention in areas V1, V2, and V4 of macaque visual cortex. J. Neurophysiol. *77*, 24–42.

Markov, N.T., Vezoli, J., Chameau, P., Falchier, A., Quilodran, R., Huissoud, C., Lamy, C., Misery, P., Giroud, P., Ullman, S., et al. (2014). Anatomy of hierarchy: feedforward and feedback pathways in macaque visual cortex. J. Comp. Neurol. *522*, 225–259.

Moran, J., and Desimone, R. (1985). Selective attention gates visual processing in the extrastriate cortex. Science *229*, 782–784.

Muthukumaraswamy, S.D., and Singh, K.D. (2013). Visual gamma oscillations: the effects of stimulus type, visual field coverage and stimulus motion on MEG and EEG recordings. Neuroimage *69*, 223–230.

Nuthmann, A., and Henderson, J.M. (2010). Object-based attentional selection in scene viewing. J. Vis. *10*, 20.

Otero-Millan, J., Troncoso, X.G., Macknik, S.L., Serrano-Pedraza, I., and Martinez-Conde, S. (2008). Saccades and microsaccades during visual fixation, exploration, and search: foundations for a common saccadic generator. J. Vis. *8*, 21.21-18.

Ray, S., and Maunsell, J.H. (2010). Differences in gamma frequencies across visual cortex restrict their possible use in computation. Neuron *67*, 885–896.

Ray, S., and Maunsell, J.H. (2011). Different origins of gamma rhythm and high-gamma activity in macaque visual cortex. PLoS Biol. *9*, e1000610.

Renart, A., de la Rocha, J., Bartho, P., Hollender, L., Parga, N., Reyes, A., and Harris, K.D. (2010). The asynchronous state in cortical circuits. Science *327*, 587–590.

Reynolds, J.H., and Chelazzi, L. (2004). Attentional modulation of visual processing. Annu. Rev. Neurosci. *27*, 611–647.

Reynolds, J.H., and Heeger, D.J. (2009). The normalization model of attention. Neuron *61*, 168–185.

Reynolds, J.H., Chelazzi, L., and Desimone, R. (1999). Competitive mechanisms subserve attention in macaque areas V2 and V4. J. Neurosci. *19*, 1736–1753.

Reynolds, J.H., Pasternak, T., and Desimone, R. (2000). Attention increases sensitivity of V4 neurons. Neuron *26*, 703–714.

Roberts, M.J., Lowet, E., Brunet, N.M., Ter Wal, M., Tiesinga, P., Fries, P., and De Weerd, P. (2013). Robust gamma coherence between macaque V1 and V2 by dynamic frequency matching. Neuron *78*, 523–536.

Roopun, A.K., Lebeau, F.E., Rammell, J., Cunningham, M.O., Traub, R.D., and Whittington, M.A. (2010). Cholinergic neuromodulation controls directed temporal communication in neocortex in vitro. Front. Neural Circuits *4*, 8.

Saalmann, Y.B., Pinsk, M.A., Wang, L., Li, X., and Kastner, S. (2012). The pulvinar regulates information transmission between cortical areas based on attention demands. Science *337*, 753–756.

Salinas, E., and Sejnowski, T.J. (2001). Correlated neuronal activity and the flow of neural information. Nat. Rev. Neurosci. *2*, 539–550.

Salkoff, D.B., Zagha, E., Yüzgeç, Ö., and McCormick, D.A. (2015). Synaptic Mechanisms of Tight Spike Synchrony at Gamma Frequency in Cerebral Cortex. J. Neurosci. *35*, 10236–10251.

Schoffelen, J.M., Oostenveld, R., and Fries, P. (2005). Neuronal coherence as a mechanism of effective corticospinal interaction. Science *308*, 111–113.

Schoffelen, J.M., Poort, J., Oostenveld, R., and Fries, P. (2011). Selective movement preparation is subserved by selective increases in corticomuscular gamma-band coherence. J. Neurosci. *31*, 6750–6758.

Schomburg, E.W., Fernández-Ruiz, A., Mizuseki, K., Berényi, A., Anastassiou, C.A., Koch, C., and Buzsáki, G. (2014). Theta phase segregation of input-specific gamma patterns in entorhinal-hippocampal networks. Neuron *84*, 470–485.

Shu, Y., Hasenstaub, A., and McCormick, D.A. (2003). Turning on and off recurrent balanced cortical activity. Nature *423*, 288–293.

Siegle, J.H., Pritchett, D.L., and Moore, C.I. (2014). Gamma-range synchronization of fast-spiking interneurons can enhance detection of tactile stimuli. Nat. Neurosci. *17*, 1371–1379.

Swettenham, J.B., Muthukumaraswamy, S.D., and Singh, K.D. (2009). Spectral properties of induced and evoked gamma oscillations in human early visual cortex to moving and stationary stimuli. J. Neurophysiol. *102*, 1241–1253.

Tan, A.Y., Chen, Y., Scholl, B., Seidemann, E., and Priebe, N.J. (2014). Sensory stimulation shifts visual cortex from synchronous to asynchronous states. Nature *509*, 226–229.

Taylor, K., Mandon, S., Freiwald, W.A., and Kreiter, A.K. (2005). Coherent oscillatory activity in monkey area v4 predicts successful allocation of attention. Cereb. Cortex *15*, 1424–1437.

Tiesinga, P.H., Fellous, J.M., Salinas, E., José, J.V., and Sejnowski, T.J. (2004). Inhibitory synchrony as a mechanism for attentional gain modulation. J. Physiol. Paris *98*, 296–314.

van Dijk, H., Schoffelen, J.M., Oostenveld, R., and Jensen, O. (2008). Prestimulus oscillatory activity in the alpha band predicts visual discrimination ability. J. Neurosci. *28*, 1816–1823.

van Ede, F., de Lange, F., Jensen, O., and Maris, E. (2011). Orienting attention to an upcoming tactile event involves a spatially and temporally specific modulation of sensorimotor alpha- and beta-band oscillations. J. Neurosci. *31*, 2016–2024.

van Elswijk, G., Maij, F., Schoffelen, J.M., Overeem, S., Stegeman, D.F., and Fries, P. (2010). Corticospinal beta-band synchronization entails rhythmic gain modulation. J. Neurosci. *30*, 4481–4488.

van Kerkoerle, T., Self, M.W., Dagnino, B., Gariel-Mathis, M.A., Poort, J., van der Togt, C., and Roelfsema, P.R. (2014). Alpha and gamma oscillations characterize feedback and feedforward processing in monkey visual cortex. Proc. Natl. Acad. Sci. USA *111*, 14332–14341.

van Pelt, S., and Fries, P. (2013). Visual stimulus eccentricity affects human gamma peak frequency. Neuroimage *78*, 439–447.

van Pelt, S., Boomsma, D.I., and Fries, P. (2012). Magnetoencephalography in twins reveals a strong genetic determination of the peak frequency of visually induced γ-band synchronization. J. Neurosci. *32*, 3388–3392.

Vinck, M., Lima, B., Womelsdorf, T., Oostenveld, R., Singer, W., Neuenschwander, S., and Fries, P. (2010). Gamma-phase shifting in awake monkey visual cortex. J. Neurosci. *30*, 1250–1257.

Vinck, M., Womelsdorf, T., Buffalo, E.A., Desimone, R., and Fries, P. (2013). Attentional modulation of cell-class-specific gamma-band synchronization in awake monkey area v4. Neuron *80*, 1077–1089.

Voloh, B., Valiante, T.A., Everling, S., and Womelsdorf, T. (2015). Theta-gamma coordination between anterior cingulate and prefrontal cortex indexes correct attention shifts. Proc. Natl. Acad. Sci. USA *112*, 8457–8462.

von Stein, A., Chiang, C., and König, P. (2000). Top-down processing mediated by interareal synchronization. Proc. Natl. Acad. Sci. USA *97*, 14748–14753.

Womelsdorf, T., Fries, P., Mitra, P.P., and Desimone, R. (2006). Gamma-band synchronization in visual cortex predicts speed of change detection. Nature *439*, 733–736.

Womelsdorf, T., Schoffelen, J.M., Oostenveld, R., Singer, W., Desimone, R., Engel, A.K., and Fries, P. (2007). Modulation of neuronal interactions through neuronal synchronization. Science *316*, 1609–1612.

Womelsdorf, T., Lima, B., Vinck, M., Oostenveld, R., Singer, W., Neuenschwander, S., and Fries, P. (2012). Orientation selectivity and noise correlation in awake monkey area V1 are modulated by the gamma cycle. Proc. Natl. Acad. Sci. USA *109*, 4302–4307.

Worden, M.S., Foxe, J.J., Wang, N., and Simpson, G.V. (2000). Anticipatory biasing of visuospatial attention indexed by retinotopically specific alpha-band electroencephalography increases over occipital cortex. J. Neurosci. *20*, RC63.

Zandvakili, A., and Kohn, A. (2015). Coordinated neuronal activity enhances corticocortical communication. Neuron *87*, 827–839.

Zhang, Y., Meyers, E.M., Bichot, N.P., Serre, T., Poggio, T.A., and Desimone, R. (2011). Object decoding with attention in inferior temporal cortex. Proc. Natl. Acad. Sci. USA *108*, 8850–8855.

Zumer, J.M., Scheeringa, R., Schoffelen, J.M., Norris, D.G., and Jensen, O. (2014). Occipital alpha activity during stimulus processing gates the information flow to object-selective cortex. PLoS Biol. *12*, e1001965.